# Northumbria Research Link

Citation: Li, Shu-Ying, Meng, Shuang, Zou, Xiaoqin, El-Roz, Mohamad, Telegeev, Igor, Thili, Oumaima, Liu, Terence and Zhu, Guangshan (2019) Rhenium-functionalized covalent organic framework photocatalyst for efficient CO2 reduction under visible light. Microporous and Mesoporous Materials, 285. pp. 195-201. ISSN 1387-1811

Published by: Elsevier

URL: https://doi.org/10.1016/j.micromeso.2019.05.026 <https://doi.org/10.1016/j.micromeso.2019.05.026>

This version was downloaded from Northumbria Research Link: http://nrl.northumbria.ac.uk/id/eprint/39544/

Northumbria University has developed Northumbria Research Link (NRL) to enable users to access the University's research output. Copyright © and moral rights for items on NRL are retained by the individual author(s) and/or other copyright owners. Single copies of full items can be reproduced, displayed or performed, and given to third parties in any format or medium for personal research or study, educational, or not-for-profit purposes without prior permission or charge, provided the authors, title and full bibliographic details are given, as well as a hyperlink and/or URL to the original metadata page. The content must not be changed in any way. Full items must not be sold commercially in any format or medium without formal permission of the copyright holder. The full policy is available online: http://nrl.northumbria.ac.uk/policies.html

This document may differ from the final, published version of the research and has been made available online in accordance with publisher policies. To read and/or cite from the published version of the research, please visit the publisher's website (a subscription may be required.)

Northumbria University NEWCASTLE

CUSTOMER SERVICE EXCELLENCE CSE UniversityLibrary

# Rhenium-Functionalized Covalent Organic Framework Photocatalyst for Efficient $CO_2$ Reduction under Visible Light

Shu-Ying Li,[#a] Shuang Meng,[#a] Xiaoqin Zou,*[a] Mohamad El-Roz,*[b] Igor Telegeev,[b] Oumaima Thili,[b] Terence Xiaoteng Liu,[c] and Guangshan Zhu~~*~~[a]

[a] Key Laboratory of Polyoxometalate Science of the Ministry of Education, Faculty of Chemistry, Northeast Normal University, Changchun 130024, P. R. China.

[b] Normandie University, Ensicaen, Unicaen, CNRS, Laboratoire Catalyse et Spectrochimie, 14000 Caen, France.

[c] Department of Mechanical & Construction Engineering, Faculty of Engineering and Environment, Northumbria University, Newcastle upon Tyne, NE1 8ST, U. K.

[#] The authors contributed equally to this work.

* Corresponding authors: zouxq100@nenu.edu.cn (X. Q. Zou), mohamad.elroz@ensicaen.fr (M. El-Roz)~~, zhugs100@nenu.edu.cn (G. S. Zhu)~~.

## Graphical Abstracts

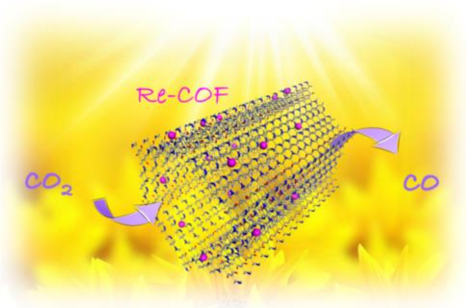


Formatted: Superscript

Formatted: Superscript

# Highlights

Covalent organic framework with monodispersed metallic catalytic site was synthesized.

It served as photocatalyst for $CO_2$ reduction with sustained lifetime up to 12 hours.

Molecular catalysis was realized in heterogeneous catalysis with a higher efficiency.

Mechanism of photocatalytic performance was explored by a new in-situ FTIR reactor.


# Abstract

The conversion of carbon dioxide ($CO_2$) into value-added chemicals under photochemical conditions has attracted increasing attention in recent years. One of the great challenges is to develop novel active catalysts under visible light irradiation with sustained lifetime and high activity. In this regard, herein, we report a highly efficient, stable and recyclable photocatalyst by embedding photoactive rhenium complex ($Re(CO)_5Cl$) into porous, crystalline, bipyridine-based covalent organic frameworks (COFs). The rhenium post-metallated COFs exhibits salient photocatalytic activity towards $CO_2$ reduction into CO under visible light. The quantity of the CO produced on Re-functionalized COFs is twice higher than that produced on the famous $Re(bpy)(CO)_3Cl$ (bpy=2,2'-bipyridine) molecular photocatalyst under similar reaction conditions.



# Keywords

2D covalent organic framework, rhenium functionalization, photocatalysis, $CO_2$ reduction, molecular catalysis.


# 1. Introduction

$CO_2$ emissions from the massive use of fossil fuels have become a serious environmental concern~~.~~[1]. Facilitating the conversion of greenhouse gas $CO_2$ into valuable chemicals like CO, $CH_4$, HCOOH, and $CH_3OH$ can tackle the issues of fossil fuel shortage and global warming at once[2-6]. Among numerous approaches for $CO_2$ transformation, reducing $CO_2$ by exploiting solar light is regarded as a promising alternative which is economical and widely available[7-14]. As is known, photocatalysts based on $Re^{I}$ bipyridine complexes $[Re^{I}(bpy)(CO)_3Cl]$ have been extensively explored as highly active photocatalysts for consuming $CO_2$ to produce CO or $HCOO^-$ under visible light[15-17]. However, molecular catalysts usually aggregate together easily during reaction process resulted in catalyst deactivation. In addition, the recycling and reuse of the catalysts from the reaction media is very difficult. Therefore, developing efficient, durable and recyclable photocatalysts for $CO_2$ reduction is of high importance.

Covalent organic frameworks (COFs) are a new class of porous materials with high crystallinity, large surface area and designable structure, which are attractive in numerous fields such as gas adsorption and separation, catalysis and molecular sensing[18-21]. The skeleton and property of COFs can be tuned by adjusting the symmetry, size and nature of building units[22, 23]. Notably, when molecular catalysts are incorporated into topological frameworks, the integration could exhibit more efficient performance than the corresponding molecular catalysts[24]. One intriguing example is that dramatic improvement of catalytic efficiency has been achieved for a polymeric ionic polymer bearing Lewis acid sites rather than its individual components[25]. Furthermore, well-defined COFs are able to provide a uniform catalytic environment which is essential for the investigation of physicochemical mechanism during reaction process. Therefore, it is promising for COFs to serve as host platforms accommodating guest active moieties and to realize cooperative functions[26].

Herein, we demonstrate the synthesis of an efficient photocatalyst with isolated, molecularly defined catalytic sites for $CO_2$ reduction to CO by loading rhenium complex ($Re(CO)_5Cl$) onto the pore walls of COFs (TpBpy) comprising rich 2,2'-bipyridine groups (Fig. 1). The modified COFs (Re-TpBpy) still preserve the crystallinity and have a high surface area, thereby offering a catalytic environment and a ready access for $CO_2$ to the catalytic sites. Anchoring rhenium complex into COFs not only facilitates a dispersive arrangement of active sites generating enhanced photocatalysis efficiency, but also prevents the losing of active species resulted in a recyclable catalyst with the long-term stability. The present results bring new enlightenments in fabricating well-defined, efficient, recyclable photocatalyst by utilizing highly ordered COFs with available chelating sites as a platform for functional moieties.

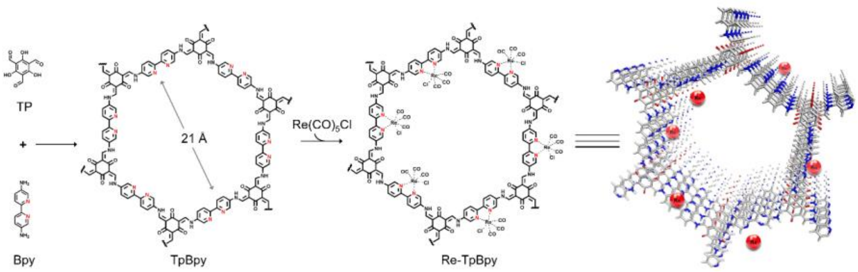


**Fig. 1.** Illustration for the construction steps of TpBpy and Re-TpBpy COFs.

## 2. Experimental section

### 2.1 Synthesis

**Synthesis of TpBpy COF**

All starting solid chemicals and solvents were obtained commercially and used without further purification. TpBpy COF was synthesized following a previous literature[27]. In brief, 1,3,5-triformylphloroglucinol (Tp) (25.2 mg) and 2,2'-bipyridine-5,5'-diamine (Bpy) (33.5 mg) were added into a pyrex tube (o.d. × i.d. = 16 × 12 $mm^2$ and length 18 cm) and dissolved in the mixture of 1.8 mL of dimethylacetamide (DMAc), 0.6 mL of o-dichlorobenzene (o-DCB) and 0.24 mL of 6.0 M aqueous acetic acid (AcOH). This reaction mixture was sonicated for 15 minutes to obtain a homogenous dispersion. The tube was flash-frozen in a liquid $N_2$ bath (77 K), degassed by three freeze-pump-thaw cycles and flame sealed. Then the mixture was heated at 120 °C and left undisturbed for 3 days, yielding a dark-red solid. Then the tube was broken at neck. The product was isolated by filtration and washed with DMAc, water and acetone. The collected powder was immersed in acetone for 12 h, during which the activation solvent was replenished three times. Finally, the product was dried at 100 ºC under vacuum for 24 h to afford TpBpy COF in 75% isolated yield.

**Synthesis of Re-TpBpy COF**

TpBpy COF (35 mg) and $Re(CO)_5Cl$ (47.9 mg) were mixed in 10 mL methanol (MeOH). The mixture was then refluxed for 24 h under $N_2$. The resultant red powder was washed with MeOH three times and collected by vacuum filtration. Finally, the product was dried at 80 °C in vacuum for 12 h.

**Synthesis of Re-Bpy Molecular Compound**

Bpy (19 mg) and $Re(CO)_5Cl$ (36.2 mg) were mixed in 10 mL methanol (MeOH). The mixture was then refluxed for 24 h under $N_2$. The resultant yellow powder was washed with MeOH three times and collected by vacuum filtration. Finally, the product was dried at 80 °C in vacuum for 12 h.

**2.2 Characterization**

FTIR spectra (KBr) were recorded on Nicolet IS50 Fourier transforms infrared spectrometer (FTIR). $N_2$ adsorption-desorption isotherms and pore size distributions were obtained at 77 K using an Autosorb iQ2 adsorptometer, Quantachrome Instrument. $CO_2$ adsorption isotherms were obtained on the same apparatus at 298 K. PXRD measurements were performed on Rigaku D/MAX2550 diffractometer using Cu-Kα (λ = 1.5418 Å) radiation running at a voltage of 40 kV and a current of 200 mA. TEM images were measured on JEOL JEM 3010. SEM imaging was implemented on field emission scanning electron microscope equipped with energy-dispersive X-ray spectroscopy (FE-SEM, SU-8010, Hitachi). The X-ray photoelectron spectroscopy (XPS) spectra were collected on a Thermo ESCALAB 250 instrument using Al-Kα as the exciting radiation (energy step size of 1.0 eV, pass energy of 20.0 eV) and binding energy calibration was based on C 1s at 284.6 eV. Metal contents in the COF were measured by ICP-OES (Inductively coupled plasma-optical emission spectrometry) on a ThermoScientificiCAP6300. The samples for ICP-OES tests were digested in aqua regia (concentrated HCl and $HNO_3$ with a volume ratio of 3:1) at 60 °C for 12 h. Then the obtained solutions were further diluted 20 times for ICP-OES tests. The Thermo-gravimetric Analysis (TGA) experiments were conducted on the Perkin Elmer thermogravimetric analyzer at a heating rate of 10 °C $min^{-1}$ in air.

### 2.3 Photocatalytic measurements

The photocatalytic $CO_2$ reduction was tested in a new in-situ reactor developed recently in the LCS laboratory and presented in Scheme 1 [28]. The reactor is made from glass and equipped with two gas inlet and outlet, perpendicular to the tubes ensuring the FTIR beam pathway through $CaF_2$ windows. The FTIR tubes are slightly tilted to prevent the solvent condensation and accumulation. The UV-visible irradiation is ensured from the top through a removable quartz window. The quartz and $CaF_2$ windows are attached to the reactor with screw fittings and the tightness is obtained by adapted Teflon O-rings. The total internal volume of the reactor is 160 ± 5 ml and can be filled with 10 to 50 ml of the solution. The design allows an easy opening and closing of the reactor, therefore, an easy clean after each experiment. The purge of the reactor is ensured by the mass flow controller system. All IR spectrum measurements with the *in situ* FTIR reactor were monitored in real time with 2 to 5 min per spectrum of time resolution. IR spectra of the reactor headspace were recorded using Nicolet 6700 IR spectrometer (Thermo Fisher Scientific) equipped with an MCT detector. All photocatalytic tests presented in this work were performed in batch configuration and at room temperature (25-30 °C). As a light source, Xe-lamp (LC8 Hamamatsu, 200 W) with pass-high filter at 390 nm was used. 15 mg of the photocatalysts was dispersed in AcN/$H_2O$ mixture (10/1.8 ml) contained 0.1 M of triethanolamine~~triethylamine~~ (TEOA) as electron donor. The solution was sonicated for 30 min at room temperature and bubbled with argon and then with saturated with $CO_2$ for 30 min with a flow rate of 20 ml min$^{-1}$.

Off-line GC (gas chromatography) analysis of CO in the headspace were conducted, at the end of the reaction, using Thermo Scientific Trace 1310 with a Thermal conductivity detector (GC-TCD for TRACE 1300 GC Series, Thermo Scientific), and equipped with a MolSive5 A column (30 m × 0.53 mm, 50 µm). For this purpose, injections (1 ml) of gas headspace were made in the GC and the resulting peak areas were converted into concentrations by using a calibration with the corresponding standard gas (operating conditions: carrier gas: He; split flow rate = 60 ml min$^{-1}$; split ratio= 1/12; inlet temperature = 423 K; column temperature 393 K).

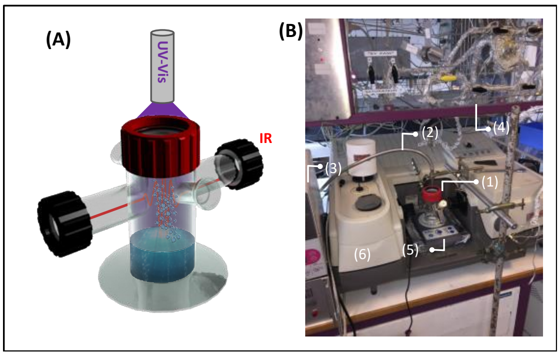


**Scheme 1.** (a) The *in-situ* FTIR reactor and (b) the entire setup used for performing the photocatalytic tests: (1) *in-situ* FTIR reactor; (2) optical fiber guide light; (3) light source; (4) gas flow setup (for purge); (5) magnetic stirrer~~steerer~~; (6) FTIR spectrometer. More details on the setup can be found in a recent reference [28].

# 3. Results and discussion

### 3.1 Characterization of the COF photocatalyst

The preparation of TpBpy COF was performed by reacting 1, 3, 5-triformylphloroglucinol (Tp) and 2,2'-bipyridine-5,5'-diamine (Bpy) *via* Schiff-base condensation according to a previously reported protocol[29]. As depicted in Fig. 2a, the experimental powder X-ray diffraction (PXRD) results are in accordance with the simulated 2D model based on AA stacking structure in the hexagonal space group (P6/m). The PXRD pattern of TpBpy exhibits an intense first peak at 2θ of 3.6°, corresponding to the reflection from (100) plane. Considering the (001) facet emerging at 25.6°, the π–π stacking interlayer distance in COF is deduced to be 3.5 Å. On the other hand, the rhenium-modified TpBpy (Re-TpBpy) was synthesized by refluxing $Re(CO)_5Cl$ with TpBpy in methanol for 24 h under $N_2$ atmosphere. The collected PXRD pattern displays the first intense peak at the same position (2θ = 3.6°) as that of TpBpy, which demonstrates the retention of the pristine framework structure of TpBpy COFs after rhenium incorporation.

$N_2$ adsorption isotherms at 77 K were measured to investigate the porosity of TpBpy and Re-TpBpy COFs (Fig. 2b). The surface area of primitive TpBpy COF is 1526 $m^2\ g^{-1}$, whereas Re-TpBpy COF exhibits a decrease in the surface area (632 $m^2\ g^{-1}$). This phenomenon is supposed to be resulted from the occupancy of partial pore spaces in Re-TpBpy COF by $Re(CO)_3Cl$ moieties and to the higher density of the Re-TpBpy in respect to the TpBpy composite. Notably, the BET surface area of Re-TpBpy is still relatively high and the porous structure is well preserved. Therefore, a high accessibility of the Re active sites in the COF channels is ensured.

Besides, the functionalization of the open N, N'-chelating sites with $Re(CO)_3Cl$ group in as-prepared Re-TpBpy was further verified by Fourier Transform Infrared (FTIR) spectroscopy (Fig. 2c). Upon complexation, two additional peaks arise at 2027 and 1903 $cm^{-1}$ in the spectrum of Re-TpBpy relative to the FT-IR peaks of TpBpy, which are assigned to the C=O stretching vibration in $Re(CO)_3Cl$ moiety. Furthermore, in the FT-IR spectrum of Re-TpBpy, the emerged C=O stretching bonds (2027 and 1903 $cm^{-1}$) and the broadened C-N peak at 1248 $cm^{-1}$ reveal a slight red shift compared with those in the starting material of $Re(CO)_5Cl$ (2043 and 1961 $cm^{-1}$) and TpBpy COF (1266 $cm^{-1}$), respectively, indicative of the formation of Re–N bonds between $Re(CO)_3Cl$ complex and 2,2'-bipyridine groups.

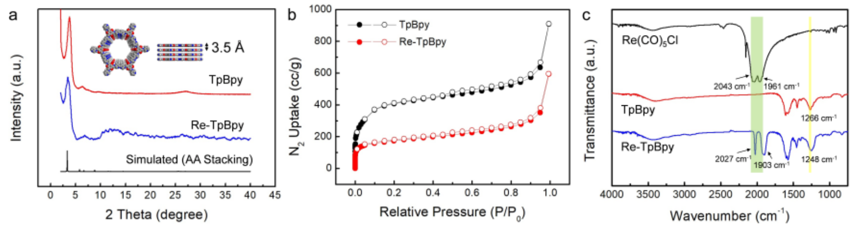


**Fig. 2.** (a) Comparative powder X-ray diffraction (PXRD) patterns; (b) $N_2$ adsorption-desorption isotherms collected at 77 K. The relative pressure ($P/P_0$) range for determination of the TpBpy BET surface area is from $1.0024\times10^{-2}$ to $1.4934\times10^{-1}$, while it is from $9.0216\times10^{-3}$ to $9.9490\times10^{-2}$ for determination of the Re-TpBpy BET surface area. (c) FT-IR spectra.

To provide additional proof, X-ray photoelectron spectroscopy (XPS) analysis was performed. The two nitrogen species in deconvoluted N 1s spectrum located at 400.19 eV and 398.99 eV are ascribed to the secondary nitrogen and pyridinic nitrogen in TpBpy, respectively (Fig. 3b)[27, 30, 31]. After TpBpy functionalization, two sets of signals corresponding to 42.54 eV and 198.22 eV are observed as shown in Fig. 3a, which are assigned to rhenium and chlorine, respectively, indicating the existence of rhenium complex in the host COF. It is noteworthy that, upon rhenium impregnation, the binding energy of pyridinic nitrogen shifts to the higher energy position from 398.99 eV to 400.46 eV (Fig. 3c), implying the coordination between rhenium and nitrogen in bipyridine. The increase of binding energy is ascribed to the decrease of electron cloud density of pyridine nitrogen, resulting from the transfer of electrons from nitrogen atoms in pyridine to the rhenium. Furthermore, the peak position of secondary nitrogen remains almost unchanged at 400.19 eV, which indicates that the rhenium complex chelates to bipyridinic units in TpBpy COF only. The total disappearance of the signal at 398.99 eV demonstrates the high yield of functionalization of the TpBpy with $Re(CO)_3Cl$ group.

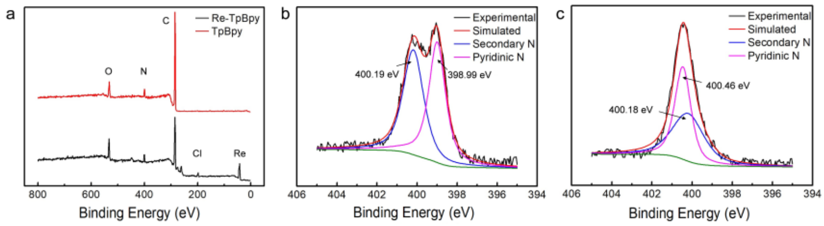


**Fig. 3.** (a) XPS survey of TpBpy and Re-TpBpy COFs, (b) and (c) correspond to the XPS N 1s spectra of TpBpy and Re-TpBpy, respectively.

The quantitative measurement acquired by inductively coupled plasma optical emission spectroscopy (ICP-OES) illustrates that the mass fraction of Re in the prepared Re-TpBpy COF is up to 26.4%. Additionally, transmission electron microscopy (TEM), scanning electron microscopy (SEM) and local energy-dispersive X-ray (EDX) spectra investigations were also carried out to further evaluate the distribution and the status of ~~Rhenium~~ rhenium in the Re-TpBpy COF. According to the electron microscopic observation, no obvious difference in the morphology could be distinguished between the parent TpBpy and the Re-functionalized TpBpy COFs (Fig. S1 in electronic supplementary information (ESI)). TEM images in Fig. 4a reveal that no metal aggregates are detected in the Re modified COF material. Moreover, EDX mapping *via* SEM confirms the homogeneous distribution of Re, N, C and O content in Re-TpBpy (Fig. 4b-f), implying a high and homogeneous dispersion of rhenium species into the Re-TpBpy COF.

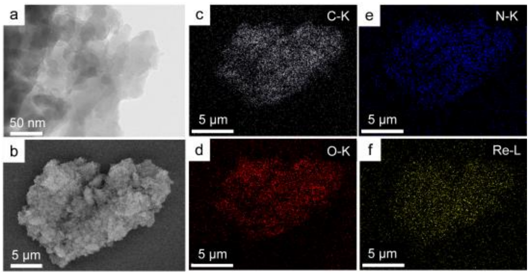


**Fig. 4.** TEM (a) and SEM (b) images, and the elemental mapping of the Re-TpBpy COF (c-f).

Since the 2, 2'-bpy fragment in the TpBpy COF is the essential part for coordination with $Re(CO)_5Cl$, the reference compound $Re(bpy)(CO)_3Cl$ (bpy = 2,2'-bipyridine) (abbreviated as Re-Bpy) was also synthesized to explore the photocatalytic mechanism in $CO_2$ reduction. FTIR spectrum (Fig. S4) and XPS characteristics (Fig. S5) of Re-Bpy can be found in ESI. After rhenium modification, there are two new peaks emerging at around 41.99 eV and 197.92 eV in deconvoluted N 1s spectrum (Fig. S5a), which are assigned to rhenium and chlorine in $Re(CO)_3Cl$ moiety, respectively, confirming the successful incorporation of rhenium complex into Bpy. Furthermore, upon rhenium impregnation, the binding energy of pyridinic nitrogen increases from 398.37 eV to 399.22 eV (Fig. S5b, c), suggesting the coordination between rhenium and nitrogen in 2, 2'-bipyridine groups. In contrast, the peak position of secondary nitrogen remains almost unchanged at 399.33 eV, implying that the coordination sites are bipyridinic units in Bpy only. ICP-OES results indicate the mass fraction of Re in the prepared Re-Bpy is about 32%.

As is known, the adsorption of $CO_2$ onto catalyst surface is prerequisite for the following catalytic process. Porous structure in the Re-TpBpy COF may facilitate the capture of $CO_2$ and play a critical role in promoting the conversion of $CO_2$ (Fig. 2b and Table S1). The impregnation of polar rhenium complex contributes to the increase of polarity of the Re-TpBpy relative to the pristine TpBpy COF, which benefits a higher adsorption ~~capacity~~ capability of $CO_2$. As depicted in Fig. 5, Re-TpBpy COF displays a $CO_2$ adsorption volume of 44 $cm^3\ g^{-1}$ at atmospheric pressure at 298 K while the $CO_2$ adsorption capability of Re-Bpy is almost zero. Additionally, the steeper uptake for $CO_2$ at low relative pressures is observed in the Re-TpBpy COF compared to that of TpBpy COF, implying a stronger interaction of $CO_2$ in Re-TpBpy (inset in Fig. 5). Both results of higher adsorption volume and stronger interaction enable the Re-TpBpy COF to serve as a more promising photocatalyst for $CO_2$ reduction.

**Formatted:** Highlight

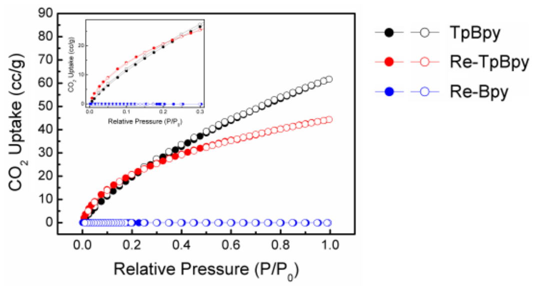


**Fig. 5.** $CO_2$ uptakes on TpBpy and Re-TpBpy COFs, and the Re-Bpy molecular compound at 298 K. The inset

image zooms on the low pressure. $P_0$ here refers to 1.0 bar.

The DR-UV-visible spectra of the different samples and the emission spectra of the visible-light source are presented in Fig. 6. A clear extension of the visible light absorbance of Re-TpBpy (600 nm take-off absorbance, Fig. 6c) in respect to Re-Bpy (~450 nm, Fig. 6a) can be observed. This is due to an increase of the electron conjugation/delocalization of the COF framework of Re-TpBpy. On the other hand, both TpBpy (Fig. 6b) and Re-TpBpy (Fig. 6c) materials show similar light absorbance behavior, demonstrating the high stability of the ligand (chromophore function) after functionalization. In our experiment, the emission wavelength maxima around 470 nm was used (Fig. 6d), which overlaps perfectly with the UV-VIS absorbance spectrum of Re-TpBpy.

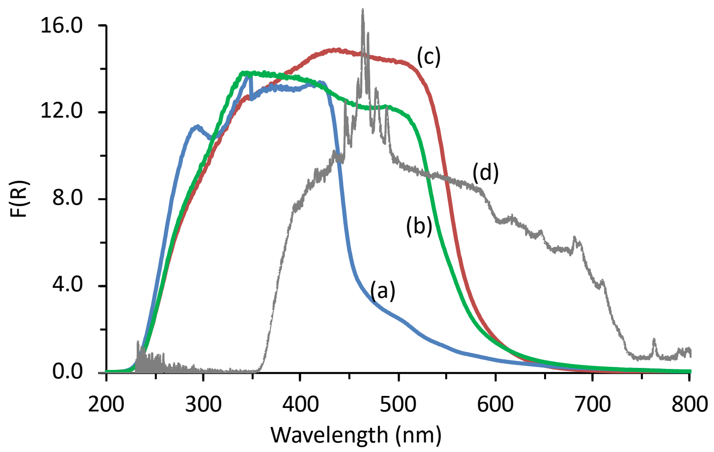


**Fig. 6.** DR-UV-visible spectra of Re-Bpy (a), TpBpy (b), and Re-TpBpy (c) samples studied in this work. (d) corresponds to the emission spectrum of the Xe-lamp (with pass-high filter at 390 nm) used in the photocatalytic test.

### 3.2 Photocatalytic $CO_2$ reduction

The $CO_2$ photoreduction was performed using a new *in situ* FTIR reactor (in a batch mode) as described in the experimental section. The photocatalysts have been tested under similar reaction condition used in the literature[28]. Re-TpBpy, Re-Bpy and TpBpy compounds were first dispersed in acetonitrile and water solution contained triethanolamine (TEOA) as electron donor. The solutions were then purged by Argon, in order to ensure an oxygen free atmosphere, and then with $^{12}CO_2$ or $^{13}CO_2$ . The catalysts were then tested under similar reaction conditions using Xe-lamp with a pass high filter (>390 nm) as visible light source. The CO production in the reaction headspace was followed by *in-situ* FTIR analysis using the IR band intensity of the characteristic CO vibrations at 2200-2100 $cm^{-1}$ (insert in Fig. 7). The results of CO production during photocatalytic $CO_2$ reduction on the different materials are displayed in Fig. 7. No CO is detected by using TpBpy materials and under inert atmosphere (Ar) for Re-TpBpy, Re-Bpy and TpBpy. This expected result shows that the ligand is not producing CO (by degradation) even after long irradiation time (12 h).

Re-Bpy and Re-TpBpy photocatalysts are both active under visible light and similar efficiency can be observed in the first hours of irradiation. After four hours of the reaction, a deviation on the CO production can be observed. The quantity of the CO produced on Re-TpBpy is twice higher than that produced on the Re-Bpy photocatalyst after 12 h of irradiation. It should be noted that in a solid/liquid phase heterogeneous reaction, the porosity of the catalyst can play a crucial role in the activity of the catalyst by insuring a high catalyst/reactant contact time. However, for the homogeneous catalytic reaction (the case of Re-Bpy), the reaction is diffusional and it is not related with the adsorbate capacity of the catalyst. Therefore, a higher contact time between the $CO_2$ and the Re active site in the case of dissolved Re-Bpy catalyst than that in dispersed Re-TpBpy catalyst can be expected in liquid phase. Nerveless, the presence of Re active sites and the $CO_2$ molecules in a well-confined environment (pores of the Re-TpBy) can enhance significantly their interactions and consequently the performance of the catalyst. This behavior can justify the similar activity in the first hour of irradiation. However, the higher decline of the activity of the Re-Bpy catalyst can probably be assigned to its relatively low stability in respect to Re-TpBpy. This stability was confirmed by a second cycle of the Re-TpBpy catalyst. The decrease of the activity after the second cycle is lower than 20% as demonstrate the analysis of the gas headspace of the reaction using the gas chromatography (Fig. 8), in agreement with the results obtained by *in-situ* FTIR analysis. This minor deactivation can due to many factors as a leaching or poisoning of ~~the~~ some Re active sites by the sub-product of the electron donor oxidation during the reaction. ICP results indicate there is little loss of Re content in the recycled Re-TpBpy. The mass fraction of Re in the recycled Re-TpBpy is about 26.0%, which is similar to that of the pristine Re-TpBpy. In addition, the crystalline structure has been well maintained in the recycled Re-TpBpy as revealed by the XRD investigation~~s~~ (~~Figure~~ Fig. S6). The cycle test can't be performed with Re-Bpy due to the complicated process of its recycling.

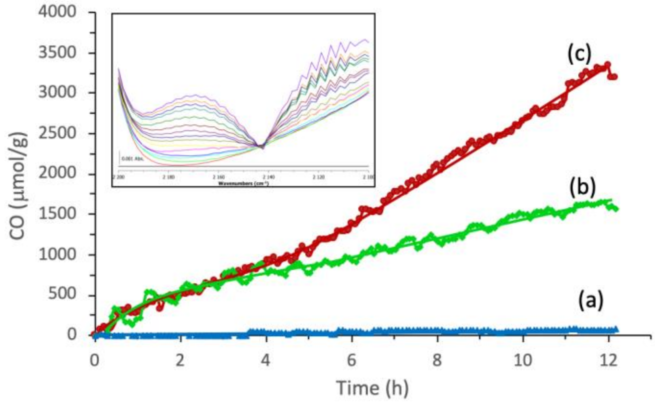


**Fig. 7.** Time course of CO production during photocatalytic $CO_2$ reduction on (a) TpBpy, (b) Re-Bpy, and (c) Re-TpBpy photocatalysts under visible light irradiation. Insert: evolution of the CO vibration band during the $CO_2$ reduction on Re-TpBpy (time resolution 1 h/spectrum). Condition: irradiation wavelength > 390 nm (see Fig. 6); Irradiance= 205 mW $cm^{-2}$; catalysts amount = 15 mg in AcN/$H_2O$ mixture (10 ml:1.8 ml); 0.1 M of TEOA.

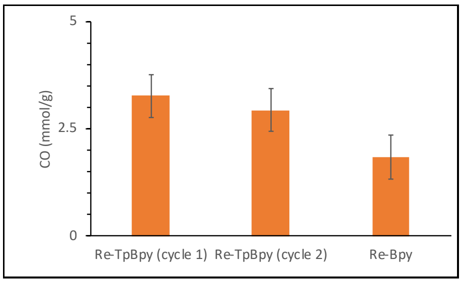


**Fig. 8.** CO produced during the $CO_2$ photoreduction on Re-TpBpy (cycle 1 and cycle 2) and Re-Bpy photocatalysts as determined by *in-situ* FTIR and GC analysis of the gas products of the reaction headspace. Reaction performed in AcN/$H_2O$ (10/1.8, ml/ml) in presence of triethanolamine (0.1 M) and 15 mg of photocatalysts under 12 h of visible light irradiation (λ>390 nm; irradiance = 205 mW $cm^{-2}$).

For confirming the origin of the CO production and the stability of the Re-TpBpy catalyst, the experiment of the $CO_2$ reduction on Re-TpBpy was repeated by using $^{13}C$ labeled $CO_2$ under the same condition used above. The FTIR spectra of the gas phase, in the stretching vibration region of CO, after 12 h of reaction using $^{12}CO_2$ and $^{13}CO_2$ are presented in ~~Figure~~ Fig. 9. Under $^{13}CO_2$, the result reveals the absence of $^{12}CO$ band (2170 $cm^{-1}$) and a selective formation of labeled $^{13}CO$ (vibration band centered at 2090 $cm^{-1}$). In addition, no formation of $^{12}CO_2$ is observed during the $^{13}CO_2$ reduction in presence of the triethanolamine, excluding any total oxidation of the ligand and/or of the electron donor. However, the partial oxidation of this later is expected and leads to the formation of dissolved acetaldehyde and water according to the literature. In summary, the photocatalyst tests demonstrate clearly the advantages of the new recyclable Re-TpBpy photocatalyst synthesized in this work for the selective $CO_2$ reduction under visible light irradiation.

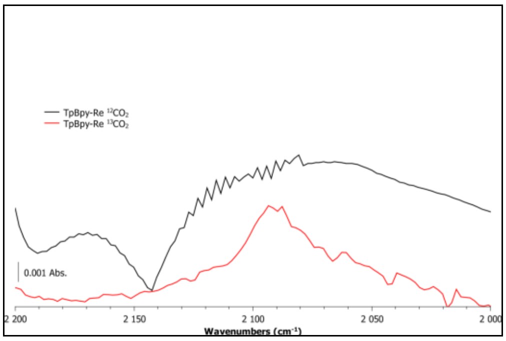


**Fig. 9**. FTIR spectra of the reaction headspace in the stretching CO vibration range after $^{12}CO_2$ (black) and $^{13}CO_2$ (red) photoreduction using Re-TpBpy as photocatalyst. Reaction performed in AcN/$H_2O$ (10/1.8, ml/ml) in presence of triethanolamine (0.1 M) and 15 mg of photocatalyst under 12 h of visible light irradiation (λ>390 nm; irradiance = 205 mW $cm^{-2}$).

## 4. Conclusions

A rhenium-functionalized COF (Re-TpBpy) was developed to serve as a recyclable catalyst with durable and high activity for photocatalytic reduction of $CO_2$ to CO. Bipyridine groups in the COF channels furnished uniform coordination sites for the chelation with metal complex, generating isolated and molecularly defined catalytic sites on the pore walls of Re-TpBpy. Experimental results revealed that the Re-TpBpy photocatalyst exhibited two times more activity than the reference compound (Re-Bpy) under the same reaction condition, and a constant increase of CO amount was observed even after 12 h of irradiation. Immobilization of metallic active center into highly-ordered COFs is proposed to be a promising approach towards $CO_2$ conversion, which not only promotes photocatalysis efficiency but also prevents the losing of active species.

## Acknowledgements

This work is supported by National Natural Science Foundation of China (21531003, 21802017), National Basic Research Program of China (973 Program, grant nos.2012CB821700, 2014CB931800), and Major International (Regional) Joint Research Project of NSFC (grant nos. 21120102034), Jilin Scientific and Technological Development Program (20170101198JC), Jilin Association of Science and Technology (2017-2018), Fundamental Research Funds for the Central Universities (2412018QD004), the China Postdoctoral Science Foundation (Grant No. 2018M631848), the Education Department of Jilin Province “13th Five-Year” Science and Technology Research (JJKH20190273KJ, JJKH20180015KJ).

## Conflict of Interest

The authors declare no conflict of interest.

## References

[1] C. Song, Catal. Today 115 (2006) 2-32.
[2] S.C. Roy, O.K. Varghese, M. Paulose, C.A. Grimes, ACS Nano 4 (2010) 1259-1278.
[3] S. Lin, C.S. Diercks, Y.-B. Zhang, N. Kornienko, E.M. Nichols, Y. Zhao, A.R. Paris, D. Kim, P. Yang, O.M. Yaghi, C.J. Chang, Science 349 (2015) 1208-1213.
[4] M. Waki, K.-i. Yamanaka, S. Shirai, Y. Maegawa, Y. Goto, Y. Yamada, S. Inagaki, Chem. Eur. J. 24 (2018) 3846-3853.
[5] W. Tu, Y. Zhou, Z. Zou, Adv. Mater. 26 (2014) 4607-4626.
[6] X. Liu, S. Inagaki, J. Gong, Angew. Chem. Int. Ed. 55 (2016) 14924-14950.
[7] S.-W. Cao, X.-F. Liu, Y.-P. Yuan, Z.-Y. Zhang, Y.-S. Liao, J. Fang, S.C.J. Loo, T.C. Sum, C. Xue,

Appl. Catal. B: Environ. 147 (2014) 940-946.
[8] K. Wang, Q. Li, B. Liu, B. Cheng, W. Ho, J. Yu, Appl. Catal. B: Environ. 176-177 (2015) 44-52.
[9] Y. Fu, D. Sun, Y. Chen, R. Huang, Z. Ding, X. Fu, Z. Li, Angew. Chem. Int. Ed. 51 (2012) 3364-3367.
[10] J.L. White, M.F. Baruch, J.E. Pander, Y. Hu, I.C. Fortmeyer, J.E. Park, T. Zhang, K. Liao, J. Gu, Y. Yan, T.W. Shaw, E. Abelev, A.B. Bocarsly, Chem. Rev. 115 (2015) 12888-12935.
[11] A.J. Morris, G.J. Meyer, E. Fujita, Acc. Chem. Res. 42 (2009) 1983-1994.
[12] R. Huang, Y. Peng, C. Wang, Z. Shi, W. Lin, Eur. J. Inorg. Chem. 2016 (2016) 4358-4362.
[13] K. Koike, D.C. Grills, Y. Tamaki, E. Fujita, K. Okubo, Y. Yamazaki, M. Saigo, T. Mukuta, K. Onda, O. Ishitani, Chem. Sci. 9 (2018) 2961-2974.
[14] X. Deng, J. Albero, L. Xu, H. García, Z. Li, Inorg. Chem. 57 (2018) 8276-8286.
[15] R. Xu, X.-S. Wang, H. Zhao, H. Lin, Y.-B. Huang, R. Cao, Catal. Sci. Technol 8 (2018) 2224-2230.
[16] H. Takeda, K. Koike, H. Inoue, O. Ishitani, J. Am. Chem. Soc. 130 (2008) 2023-2031.
[17] J.M. Smieja, C.P. Kubiak, Inorg. Chem. 49 (2010) 9283-9289.
[18] H. Liao, H. Wang, H. Ding, X. Meng, H. Xu, B. Wang, X. Ai, C. Wang, J. Mater. Chem. A, 4 (2016) 7416-7421.
[19] J.L. Segura, M.J. Mancheno, F. Zamora, Chem. Soc. Rev. 45 (2016) 5635-5671.
[20] Q. Lu, Y. Ma, H. Li, X. Guan, Y. Yusran, M. Xue, Q. Fang, Y. Yan, S. Qiu, V. Valtchev, Angew. Chem. Int. Ed. 57 (2018) 6042-6048.
[21] X. Han, Q.C. Xia, J.J. Huang, Y. Liu, C.X. Tan, Y. Cui, J. Am. Chem. Soc. 139 (2017) 8693-8697.
[22] S.-Y. Ding, W. Wang, Chem. Soc. Rev. 42 (2013) 548-568.
[23] N. Huang, P. Wang, D.L. Jiang, Nat. Rev. Mater. 1 (2016) 16068.
[24] C. Wang, Z. Xie, K.E. deKrafft, W. Lin, J. Am. Chem. Soc. 133 (2011) 13445-13454.
[25] Q. Sun, B. Aguila, J. Perman, N. Nguyen, S. Ma, J. Am. Chem. Soc. 138 (2016) 15790-15796.
[26] A.J. Blake, N.R. Champness, T.L. Easun, D.R. Allan, H. Nowell, M.W. George, J. Jia, X.-Z. Sun, Nat. Chem. 2 (2010) 688.
[27] H.B. Aiyappa, J. Thote, D.B. Shinde, R. Banerjee, S. Kurungot, Chem. Mater. 28 (2016) 4375-4379.
[28] I. Telegeiev, O. Thili, A. Lanel, P. Bazin, Y. Levaque, C. Fernandez, M. El-Roz, Anal. Chem. 90 (2018) 14586-14592.
[29] D.B. Shinde, H.B. Aiyappa, M. Bhadra, B.P. Biswal, P. Wadge, S. Kandambeth, B. Garai, T. Kundu, S. Kurungot, R. Banerjee, J. Mater. Chem. A 4 (2016) 2682-2690.
[30] S. Chandra, T. Kundu, K. Dey, M. Addicoat, T. Heine, R. Banerjee, Chem. Mater. 28 (2016) 1489-1494.
[31] R. Zhao, X. Li, B. Sun, M. Shen, X. Tan, Y. Ding, Z. Jiang, C. Wang, Chem. Eng. J. 268 (2015) 290-299.